Analysis of non-axisymmetric wave propagation in a homogeneous piezoelectric solid circular cylinder of transversely isotropic material

Michael Y. Shatalov[a]*, Arthur G. Every[b],
Alfred S. Yenwong-Fai[c]

[a] *Sensor Science and Technology (SST) of the CSIR Material Science and Manufacturing, P.O. Box 395, Pretoria 0001, CSIR, South Africa,*
Department of Mathematics and Statistics of Tshwane University of Technology, P.B.X680, Pretoria 0001 FIN-40014, TUT, South Africa.
[b] *School of Physics, University of Witwatersrand, P.O. Box 2050, Johannesburg, South Africa.*
[c] *Sensor Science and Technology (SST) of the CSIR Material Science and Manufacturing, P.O. Box 395, Pretoria 0001, CSIR, South Africa,*
School of Physics, University of Witwatersrand, P.O. Box 2050, Johannesburg, South Africa.

Abstract

A study concerning the propagation of free non-axisymmetric waves in a homogeneous piezoelectric cylinder of transversely isotropic material with axial polarization is carried out on the basis of the linear theory of elasticity and linear electromechanical coupling. The solution of the three dimensional equations of motion and quasi-electrostatic equation is given in terms of seven mechanical and three electric potentials. The characteristic equations are obtained by the application of the mechanical and two types of electric boundary conditions at the surface of the piezoelectric cylinder. A novel method of displaying dispersion curves is described in the paper and the resulting dispersion curves are presented for propagating and evanescent waves for PZT-4 and PZT-7A piezoelectric ceramics for circumferential wave numbers m = 1, 2, and 3. It is observed that the dispersion curves are sensitive to the type of the imposed boundary conditions as well as to the measure of the electromechanical coupling of the material.

Key words: Non-axisymmetric wave propagation, Piezoelectricity, Transversely isotropic material, Dispersion curves

* Corresponding author. Tel: +27128412974; fax: +27128413895
Email address: mshatlov@csir.co.za

1 Introduction

Ultrasonic non-destructive evaluation relies on a thorough understanding of the propagating and evanescent waves in the material under investigation. This study could be useful in such applications, for example, in the identification of defects of finite size across the circumference of a piezoelectric rod, since reflections of waves from such defects are generally non-axisymmetric in nature Rose, (1999). Also, results obtained in this paper can serve as a basis for design of piezoelectric transducers, for which standing wave modes resulting from reflections of travelling waves at cross-section boundaries of the cylinder play an important role. The broad development of the finite (FEM) and boundary element methods (BEM) also needs some reference results obtained from exact solutions. In this case the proposed investigation of the non-axisymmetric propagating and evanescent waves in a piezoelectric cylinder could help to create reliable test beds of FEM and BEM.

The study of wave propagation in systems with cylindrical geometry has been undertaken by a number of investigators. While the systems considered so far have been both isotropic and anisotropic in nature, a relatively larger literature exists for isotropic materials. The first investigator of waves propagating in a solid isotropic cylinder was Pochhammer (1876). Other investigators of the subject can be found in standard texts such as Achenbach (1984), Graff (1991), and Rose (1999). For cylinders composed of anisotropic materials Chree (1890) investigated propagation of the axisymmetric waves. Much later Mirsky (1964) investigated a problem of non-axisymmetric wave propagation in transversely isotropic circular solid and hollow cylinders. Other contributors to the subject were Armenakas and Reitz (1973), Frazer (1980), Nayfeh and Nagy (1995), Berliner and Solecki (1996), Niklasson and Datta (1998), and Honarvar, *et. al.* (2007), just to name a few. Numerical results for the dispersion of axisymmetric guided waves in a composite cylinder with a transversely isotropic core were presented by Xu and Datta (1991).

For piezoelectric cylinders the analysis of vibrations of circular shells was performed by Paul (1966). Investigation of axisymmetric waves in layered piezoelectric rods with open circuit electric field conditions and their composites was carry out by Nayfeh *et. al.* (2000). The axisymmetric problem of the wave propagation in a piezoelectric transversely isotropic rod was analysed for rigid sliding and elastic simply supported mechanical boundary conditions and different types of electric field conditions by Wei and Su (2005). Several papers were devoted to development of numerical and finite element methods of investigation of piezoelectric cylinders. Siao *et. al.* (1994) solved the problem of wave propagation in a laminated piezoelectric cylinder via the FEM. Their paper contains tables and graphs of dispersion curves for real and imaginary values of wavenumbers. Unfortunately the data contains a misprint in a scale factor for the dimensionless wave number, making it quite difficult to compare their results with the results of the present paper. This misprint was further corrected by Bai *et. al.* (2004), who in their paper studied the electromechanical response of a laminated piezoelectric hollow cylinder by means of a semi-analytical FEM formulation. Shatalov and Loveday (2004), Bai *et. al.* (2006) also studied the phenomenon of end reflections of waves in a semi-infinite layered piezoelectric cylinder.

Our approach parallels that of Mirsky (1964) and Berliner and Solecki (1996). It is also similar to that used by Winkel *et. al.* (1995) who analytically solved the problem of wave propagations in an infinite cylindrical piezoelectric core rod immersed into an infinite piezoelectric cladding material. Winkel *et. al.* (1995) focused on the pure guided waves with real solutions of the determining bi-cubic equation. It was found in the process of investigation that this approach is applicable to the general problem of propagating and evanescent waves with real and complex solutions. Unfortunately the paper of Winkel *et. al.* (1995) contains some misprints which do not make it possible to realize the algorithm numerically. In our approach the three dimensional equations of elastodynamics together with the quasi-electrostatic Gauss law are solved in terms of seven displacement and three electric potentials, each satisfying the Helmholtz equations. In contrast to Winkel *et. al.* (1995) we propose a simple approach to solution of the problem which has an additional advantage that in the limiting case of small electric and electromechanical constants our results automatically coincide with the classical results of Mirsky (1964) and Berliner and Solecki (1996) for a transversely isotropic cylinder. This circumstance gives one confidence in the correctness of the results obtained in this paper. Imposing the allowed mechanical and electric boundary conditions on the cylinder surface, the characteristic or dispersion equation is obtained in the form of a determinant of the fourth order.

On the basis of the obtained results a numerical algorithm for displaying the dispersion curves is developed. The algorithm is based on calculation of the logarithm of modulus of the left hand side of the dispersion equation on a discrete mesh in the "wavenumber – frequency" - ($k-\omega$) plane. If the left hand side value of the dispersion equation tends to zero the logarithm tends to minus infinity. This method produces sharp negative spikes on the surface plot and automatically provides a picture of configuration of the dispersion curves. Similar approach of simultaneous qualitative displaying of the dispersion equation solutions was used by Honarvar *et. al.* (2006) that produced a 3-D cross-section of the real part of left hand side of the equation. The main advantage of our approach is that the local minima of the logarithm of modulus of the left hand side of the dispersion equation's matrix give proper approximations of the roots which can be further used as guess values of solutions of the dispersion equation. The same approach is used for simultaneous displaying of the "wavenumber - phase velocity" – ($k-V_{ph}$) distribution diagram. In the present paper we present the dispersion curves of solid cylinders made from two piezoelectric materials – PZT-4 and PZT-7A for open- and short-circuit electric boundary conditions and for different circumferential wavenumbers m = 1, 2, and 3. The phase velocities are represented for the abovementioned piezoelectric materials for m = 1. The curves demonstrate substantial influence of the electric boundary conditions and electromechanical coupling on behaviour of the dispersion curves and phase velocities. These results obtained from exact solution of the problem could serve as the reference data and help researchers to create reliable FEM techniques for analysis of vibration of piezoelectric bodies.

2 Analytic Formulation and Solution

In this section we establish the equations of motion and boundary conditions, and obtain solution of the problem within the framework of the following assumptions and approximations: linear elasticity, linear constitutional model of piezoelectricity, quasi-

static approximation of the electric field, axial polarization of the piezoelectric material, neglecting of thermal effects, absence of free charges in the material, and boundary and body forces. Axis Oz coincides with the axis of the cylinder, r,θ,z - radius, polar angle and axial coordinate, and u,v,w - radial, tangential and axial displacements correspondingly.

Navier equations of motion and Gauss' law in cylindrical coordinates are:

$$\begin{aligned}
&\frac{\partial\sigma_1}{\partial r}+\frac{1}{r}\frac{\partial\sigma_6}{\partial\theta}+\frac{\partial\sigma_5}{\partial z}+\frac{\sigma_1-\sigma_2}{r}=\rho\ddot{u}, && \frac{\partial\sigma_6}{\partial r}+\frac{1}{r}\frac{\partial\sigma_2}{\partial\theta}+\frac{\partial\sigma_4}{\partial z}+\frac{2\sigma_6}{r}=\rho\ddot{v},\\
&\frac{\partial\sigma_5}{\partial r}+\frac{1}{r}\frac{\partial\sigma_4}{\partial\theta}+\frac{\partial\sigma_3}{\partial z}+\frac{\sigma_5}{r}=\rho\ddot{w}, && \frac{\partial D_1}{\partial r}+\frac{D_1}{r}+\frac{1}{r}\frac{\partial D_2}{\partial\theta}+\frac{\partial D_3}{\partial z}=0
\end{aligned} \tag{1}$$

where $\sigma_1=\sigma_{rr}$, $\sigma_2=\sigma_{\theta\theta}$, $\sigma_3=\sigma_{zz}$, $\sigma_4=\sigma_{z\theta}=\sigma_{\theta z}$, $\sigma_5=\sigma_{rz}=\sigma_{zr}$, $\sigma_6=\sigma_{r\theta}=\sigma_{\theta r}$ are the stresses, $D_{1,2,3}$ are the electric displacement components, and the double dot notation means second time derivative.

The coupled constitutive equations of the system in the Voigt notation are as follows:

$$\begin{aligned}
&\sigma_1=c_{11}^E S_1+c_{12}^E S_2+c_{13}^E S_3-e_{31}E_3, && \sigma_2=c_{12}^E S_1+c_{11}^E S_2+c_{13}^E S_3-e_{31}E_3,\\
&\sigma_3=c_{13}^E\left(S_1+S_2\right)+c_{13}^E S_3-e_{33}E_3, && \sigma_4=c_{44}^E S_4-e_{15}E_2,\\
&\sigma_5=c_{44}^E S_5-e_{15}E_1, && \sigma_6=c_{66}^E S_6,\\
&D_1=\varepsilon_{11}^S E_1+e_{15}S_5, && D_2=\varepsilon_{11}^S E_2+e_{15}S_4,\\
&D_3=\varepsilon_{33}^S E_3+e_{31}\left(S_1+S_2\right)+e_{33}S_3
\end{aligned} \tag{2}$$

where $S_1=S_{rr}$, $S_2=S_{\theta\theta}$, $S_3=S_{zz}$, $S_4=S_{z\theta}=S_{\theta z}$, $S_5=S_{rz}=S_{zr}$, $S_6=S_{r\theta}=S_{\theta r}$ are the strains, $E_{1,2,3}$ the electric field components, $c_{11}^E,\ldots,c_{66}^E$ the elastic stiffnesses at constant electric field $\left(c_{66}^E=0.5\left(c_{11}^E-c_{12}^E\right)\right)$, $e_{15},\ldots,e_{33}$ the piezoelectric constants or electromechanical coupling factors, and $\varepsilon_{11}^S,\varepsilon_{33}^S$ are the clamped dielectric constants at constant strain.

The strains and electric field in cylindrical coordinates are:

$$\begin{aligned}
&S_1=\frac{\partial u}{\partial r}, && S_2=\frac{1}{r}\left(u+\frac{\partial v}{\partial\theta}\right), && S_3=\frac{\partial w}{\partial z},\\
&S_4=\frac{\partial v}{\partial z}+\frac{1}{r}\frac{\partial w}{\partial\theta}, && S_5=\frac{\partial w}{\partial r}+\frac{\partial u}{\partial z}, && S_6=\frac{1}{r}\left(\frac{\partial u}{\partial\theta}-v\right)+\frac{\partial v}{\partial r},\\
&E_1=-\frac{\partial\varphi}{\partial r}, && E_2=-\frac{1}{r}\frac{\partial\varphi}{\partial\theta}, && E_3=-\frac{\partial\varphi}{\partial z}
\end{aligned} \tag{3}$$

where φ is an electric potential.

We seek the solution of the problem (1) – (3) in terms of harmonic travelling waves (since the Hook law is obeyed) along z - axis in terms of several displacement and electric potentials first introduced by Mirsky (1964) and further used by Winkel *et. al.* (1995) as follows:

$$u=\left[\sum_{j=1}^{N}\frac{\partial\Phi_j}{\partial r}+\frac{1}{r}\frac{\partial\Phi_{N+1}}{\partial\theta}\right]e^{i(\omega t+k z)},\qquad v=\left[\frac{1}{r}\sum_{j=1}^{N}\frac{\partial\Phi_j}{\partial\theta}-\frac{\partial\Phi_{N+1}}{\partial r}\right]e^{i(\omega t+k z)},$$
$$w=\left[\sum_{j=N+2}^{2N+1}\Phi_j\right]e^{i(\omega t+k z)},\qquad \varphi=\left[\sum_{j=2N+2}^{3N+1}\Phi_j\right]e^{i(\omega t+k z)} \tag{4}$$

where $\Phi=\Phi(r,\theta)$, N is chosen in the process of solution of the problem (it will be shown that for complete solution $N=3$), $i^2=-1$, ω is the angular frequency, and k is the wavenumber (real for propagating and imaginary or complex for evanescent waves).

After substitution Eqn. (4) in (3) and further in (2) and (1) the following system of equations is obtained:

$$\begin{aligned}
&\frac{\partial}{\partial r}\left\{\sum_{j=1}^{N}\left[c_{11}^{E}\nabla^2\Phi_j+\left(\rho\omega^2-k^2c_{44}^{E}\right)\Phi_j\right]+ik\left(c_{13}^{E}+c_{44}^{E}\right)\sum_{j=N+2}^{2N+1}\Phi_j+ik\left(e_{15}+e_{31}\right)\sum_{j=2N+2}^{3N+1}\Phi_j\right\}\\
&+\frac{1}{r}\frac{\partial}{\partial\theta}\left\{c_{66}^{E}\nabla^2\Phi_{N+1}+\left(\rho\omega^2-k^2c_{44}^{E}\right)\Phi_{N+1}\right\}=0,\\
&\frac{1}{r}\frac{\partial}{\partial\theta}\left\{\sum_{j=1}^{N}\left[c_{11}^{E}\nabla^2\Phi_j+\left(\rho\omega^2-k^2c_{44}^{E}\right)\Phi_j\right]+ik\left(c_{13}^{E}+c_{44}^{E}\right)\sum_{j=N+2}^{2N+1}\Phi_j+ik\left(e_{15}+e_{31}\right)\sum_{j=2N+2}^{3N+1}\Phi_j\right\}\\
&-\frac{\partial}{\partial r}\left\{c_{66}^{E}\nabla^2\Phi_{N+1}+\left(\rho\omega^2-k^2c_{44}^{E}\right)\Phi_{N+1}\right\}=0,\\
&ik\left(c_{13}^{E}+c_{44}^{E}\right)\sum_{j=1}^{N}\nabla^2\Phi_j+\sum_{j=N+2}^{2N+1}\left[c_{44}^{E}\nabla^2\Phi_j+\left(\rho\omega^2-k^2c_{33}^{E}\right)\Phi_j\right]+\sum_{j=2N+2}^{3N+1}\left[e_{15}\nabla^2\Phi_j-k^2e_{33}\Phi_j\right]=0,\\
&ik\left(e_{15}+e_{31}\right)\sum_{j=1}^{N}\nabla^2\Phi_j+\sum_{j=N+2}^{2N+1}\left[e_{15}\nabla^2\Phi_j-k^2e_{33}\Phi_j\right]-\sum_{j=2N+2}^{3N+1}\left[\varepsilon_{11}\nabla^2\Phi_j-k^2\varepsilon_{33}\Phi_j\right]=0
\end{aligned} \tag{5}$$

where $\nabla^2=\frac{\partial^2}{\partial r^2}+\frac{1}{r}\frac{\partial}{\partial r}+\frac{1}{r^2}\frac{\partial^2}{\partial\theta^2}$ is the two dimensional Laplace operator in polar coordinates.

The first two equations of the system are satisfied if

$$\begin{aligned}
&\sum_{j=1}^{N}\left[c_{11}^{E}\nabla^2\Phi_j+\left(\rho\omega^2-k^2c_{44}^{E}\right)\Phi_j\right]+ik\left(c_{13}^{E}+c_{44}^{E}\right)\sum_{j=N+2}^{2N+1}\Phi_j+ik\left(e_{15}+e_{31}\right)\sum_{j=2N+2}^{3N+1}\Phi_j=0,\\
&c_{66}^{E}\nabla^2\Phi_{N+1}+\left(\rho\omega^2-k^2c_{44}^{E}\right)\Phi_{N+1}=0
\end{aligned} \tag{6}$$

It follows from this system that the second equation is separated and the first one must be compatible with third and fourth equations of system (5). For compatibility it is possible to introduce the following representation:

$$\Phi_j = \eta_{j-(N+1)}\Phi_{j-(N+1)} \quad (j = N+2,\ldots,2N+1)$$
$$\Phi_l = \mu_{l-(2N+1)}\Phi_{l-(2N+1)} \quad (l = 2N+2,\ldots,3N+1) \tag{7}$$

where coefficients η, μ are found so that the first equation (6), third, and fourth equations (5) become compatible. It can be done by assumption that all potentials Φ_j satisfy the Helmholtz equations

$$\nabla^2\Phi_j + \xi_j^2\Phi_j = 0 \tag{8}$$

and hence, $\nabla^2\Phi_j = -\xi_j^2\Phi_j$ ($j = 1,2,\ldots,N$).

From the system of three equations the following bi-cubic determining equation is obtained:

$$\left(\xi_j^2\right)^3 + b_1\left(\xi_j^2\right)^2 + b_2\left(\xi_j^2\right) + b_3 = 0 \tag{9}$$

where

$$b_1 = \frac{-\rho\omega^2 B_1 + k^2 B_2}{B_0}; \qquad b_2 = \frac{\varepsilon_{11}\left(\rho\omega^2\right)^2 - k^2\left(\rho\omega^2\right)B_3 + k^4 B_4}{B_0},$$
$$b_3 = \frac{k^2\left(k^2 c_{44}^E - \rho\omega^2\right)\left[k^2 B_5 - \left(\rho\omega^2\right)\varepsilon_{33}\right]}{B_0}, \qquad B_0 = c_{11}^E\left(e_{15}^2 + \varepsilon_{11}c_{44}^E\right),$$
$$B_1 = e_{15}^2 + \varepsilon_{11}\left(c_{11}^E + c_{44}^E\right), \qquad B_3 = \varepsilon_{11}\left(c_{33}^E + c_{44}^E\right) + \varepsilon_{33}\left(c_{11}^E + c_{44}^E\right) + \left(e_{15} + e_{31}\right)^2 + 2e_{15}e_{33},$$
$$B_2 = \varepsilon_{11}\left(c_{11}^E c_{33}^E - 2c_{13}^E c_{44}^E - \left(c_{13}^E\right)^2\right) + 2e_{15}\left(c_{11}^E e_{33} - c_{13}^E e_{31}\right) + c_{44}^E\left(e_{31}^2 + \varepsilon_{33}c_{11}^E\right) - 2c_{13}^E e_{15}^2,$$
$$B_4 = -\left(c_{13}^E\right)^2\varepsilon_{33} - 2c_{13}^E\left[e_{33}\left(e_{15} + e_{31}\right) + c_{44}^E\varepsilon_{33}\right] + c_{33}^E\left[\left(e_{15} + e_{31}\right)^2 + c_{44}^E\varepsilon_{11} + c_{11}^E\varepsilon_{33}\right] + c_{11}^E e_{33}^2 - 2c_{44}^E e_{31}e_{33},$$
$$B_5 = c_{33}^E\varepsilon_{33} + e_{33}^2 \tag{10}$$

In the general case there are three roots to Eqn. (9) and hence, $N = 3$ because there are only three independent equations (8) and according to (7) $\Phi_5 = \eta_1\Phi_1$, $\Phi_6 = \eta_2\Phi_2$, $\Phi_7 = \eta_3\Phi_3$, $\Phi_8 = \mu_1\Phi_1$, $\Phi_9 = \mu_2\Phi_2$, and $\Phi_{10} = \mu_3\Phi_3$ where

$$\eta_j = -\frac{i}{k}\frac{\xi_j^4 c_{11}^E e_{15} + \xi_j^2\left[k^2 B_6 - \left(\rho\omega^2\right)e_{15}\right] + k^2\left(k^2 c_{44}^E - \rho\omega^2\right)e_{33}}{k^2 B_7 + \xi_j^2 B_8 + \left(\rho\omega^2\right)B_9},$$
$$\mu_j = \frac{\xi_j^2\left(\eta_j e_{15} - ikB_9\right) + k^2\eta_j e_{33}}{\xi_j^2\varepsilon_{11} + k^2\varepsilon_{33}}, \qquad (j = 1,2,3) \tag{11}$$
$$B_6 = c_{11}^E e_{33} - c_{13}^E e_{15} - \left(c_{13}^E + c_{44}^E\right)e_{31}, \qquad B_7 = \left(c_{13}^E + c_{44}^E\right)e_{33} - c_{33}^E\left(e_{15} + e_{31}\right),$$
$$B_8 = c_{13}^E e_{15} - c_{44}^E e_{31}, \qquad B_9 = e_{15} + e_{31}$$

Hence expressions (4) are as follows:

$$u=\left[\frac{\partial\Phi_1}{\partial r}+\frac{\partial\Phi_2}{\partial r}+\frac{\partial\Phi_3}{\partial r}+\frac{1}{r}\frac{\partial\Phi_4}{\partial\theta}\right]e^{i(\omega t+kz)},\quad w=\left[\eta_1\Phi_1+\eta_2\Phi_2+\eta_3\Phi_3\right]e^{i(\omega t+kz)}$$
$$v=\left[\frac{1}{r}\left(\frac{\partial\Phi_1}{\partial\theta}+\frac{\partial\Phi_2}{\partial\theta}+\frac{\partial\Phi_3}{\partial\theta}\right)-\frac{\partial\Phi_4}{\partial r}\right]e^{i(\omega t+kz)},\quad \varphi=\left[\mu_1\Phi_1+\mu_2\Phi_2+\mu_3\Phi_3\right]e^{i(\omega t+kz)} \qquad (12)$$

For the fourth equation $\nabla^2\Phi_4+\xi_4^2\Phi_4=0$ it follows from the second expression (6) that

$$\xi_4^2=\frac{\rho\omega^2-k^2c_{44}^E}{c_{66}^E} \qquad (13)$$

Solutions of the Helmholtz equations (8) and second Eqn.(6) are as follows:

$$\Phi_j(r,\theta)=A_jW_m(\xi_j r)\cos(m\theta+\theta_0),\quad (j=1,2,3)$$
$$\Phi_4(r,\theta)=A_4W_m(\xi_4 r)\sin(m\theta+\theta_0) \qquad (14)$$

where $W_m(\xi r)=J_m(\xi r)$ is the Bessel function if ξ is real or complex, $W_m(\xi r)=I_m(|\xi| r)$ is the Bessel function of the second kind if ξ id pure imaginary, m is the integer circumferential wave number, and the A (real or complex) are amplitudes.

Mechanical boundary conditions correspond to the assumption of absence of external forces on the cylindrical boundary:

$$\sigma_1\big|_{r=a}=\sigma_5\big|_{r=a}=\sigma_6\big|_{r=a}=0 \qquad (15)$$

There are two types of electric boundary conditions:

$$D_1\big|_{r=a}=0 \qquad \text{or} \qquad \varphi\big|_{r=a}=0 \qquad (16)$$

where the first expression corresponds to the open-circuit condition and the second expression – to the close-circuit condition.

After substitution (14) into (12), (3), and (2) we obtain two systems of four linear homogeneous algebraic equations in the unknown amplitudes $A_{1,\ldots,4}$. Each of these systems of equations has a non-trivial solution if and only if its main determinant equals zero:

$$Det = \begin{vmatrix} a_{11} & a_{12} & a_{13} & a_{14} \\ a_{21} & a_{22} & a_{23} & a_{24} \\ a_{31} & a_{32} & a_{33} & a_{34} \\ a_{41} & a_{42} & a_{43} & a_{44} \end{vmatrix} = 0 \tag{17}$$

Where $a_{ij} = a_{ij}(k, \omega)$ are given in the Appendix. Eqn.(17) forms the dispersion equation.

Remark on limiting case of small electro-mechanical coupling coefficients. If electro-mechanical coupling coefficients $e_{15} = e_{31} = e_{33} = 0$ the determining Eqn. (9) is converted into

$$\left[\left(\xi_j^2 \right) - k^2 \frac{\varepsilon_{33}}{\varepsilon_{11}} \right] \left[\left(\xi_j^2 \right)^2 + b_4 \left(\xi_j^2 \right) + b_5 \right] = 0 \tag{18}$$

where

$$b_4 = \frac{-\rho\omega^2 B_{11} + k^2 B_{12}}{B_{10}}, \qquad b_5 = \frac{\left(\rho\omega^2 - k^2 c_{33}^E \right)\left(\rho\omega^2 - k^2 c_{44}^E \right)}{B_{10}}, \qquad B_{10} = c_{11}^E c_{44}^E,$$
$$B_{11} = c_{11}^E + c_{44}^E, \qquad B_{12} = c_{11}^E c_{33}^E - \left(c_{13}^E \right)^2 - 2 c_{13}^E c_{44}^E \tag{19}$$

Hence in (18) the electric and mechanical parts are separated and the determining equation $\left(\xi_j^2 \right)^2 + b_4 \left(\xi_j^2 \right) + b_5 = 0$ describes the wave dynamics in the passive transversely isotropic medium. This equation coincides with the corresponding equation found by Berliner and Solecki (1996) and hence, all the results of the present paper are converted into the well known results of Mirsky (1964), and Berliner and Solecki (1996) in the limiting case of small electro-mechanical coupling coefficients. Additional dispersion lines, corresponding to $\left(\xi_j^2 \right) \varepsilon_{11} - k^2 \varepsilon_{33} = 0$ could be considered as artefacts in this case.
Furthermore if we suppose that $e_{15} = e_{31} = 0$ in the first expression (11) we obtain that

$$\eta_j = \frac{i}{k} \frac{\rho\omega^2 - \xi_j^2 c_{11}^E - k^2 c_{44}^E}{c_{13}^E + c_{44}^E}$$

which also coincides with the result of Berliner and Solecki (1996). Hence, the results obtained contain the classical results of investigation of a passive transversely isotropic material as a particular limiting case.

3 Numerical Results and Discussion

In this section we present the dispersion curves for non-axisymmetric waves with circumferential wavenumbers $m = 1, 2, 3$ resulting from the characteristic equation (17). Two piezoelectric materials are chosen, PZT-4 and PZT-7A, to illustrate the influence of electro-mechanical coupling coefficients on the configuration of the

dispersion curves. The relevant material parameters for PZT-4 and PZT-7A are given in the Table.

Geometric and Material Constants	PZT-4	PZT-7A	SI Units
Radius (a)	1	1	m
ρ	$7.5\cdot10^{3}$	$7.6\cdot10^{3}$	kg/m^{-3}
c_{11}^{E}	$13.9\cdot10^{10}$	$14.8\cdot10^{10}$	N/m^{-2}
c_{12}^{E}	$7.78\cdot10^{10}$	$7.62\cdot10^{10}$	N/m^{-2}
c_{13}^{E}	$7.43\cdot10^{10}$	$7.42\cdot10^{10}$	N/m^{-2}
c_{33}^{E}	$11.5\cdot10^{10}$	$13.1\cdot10^{10}$	N/m^{-2}
c_{44}^{E}	$2.56\cdot10^{10}$	$2.53\cdot10^{10}$	N/m^{-2}
e_{15}	12.7	9.2	C/m^{-2}
e_{31}	-5.2	-2.1	C/m^{-2}
e_{33}	15.1	9.5	C/m^{-2}
ε_{11}^{S}	$730\cdot\varepsilon_0$	$460\cdot\varepsilon_0$	$C^2m^{-2}N^{-1}$
ε_{33}^{S}	$635\cdot\varepsilon_0$	$235\cdot\varepsilon_0$	$C^2m^{-2}N^{-1}$

Table. Material constants and geometric parameters for PZT-4 and PZT-7A
$\left(\varepsilon_0 = 8.85\cdot10^{-12} \quad C^2m^{-2}N^{-1}\right)$

In order to obtain the dispersion curves we made use of a method similar to the novel method described by Honarvar *et al.* (2008) where the dispersion curves are not produced as a result of solving of the dispersion equation by a traditional iterative find-root algorithm but are obtained by a zero-level cut in the velocity-frequency plane. In our approach, we modify this approach calculating the logarithm of modulus of determinant (17) on the mesh $\left(k_i, \omega_j\right), i = 1,\ldots,N_1;\ j = 1,\ldots,N_2$. In those points where the real and imaginary parts of determinant (17) are close to zero substantial negative spikes occurwhich are displayed on a surface plot and give a picture of the configuration of the dispersion curves. The main advantage of this approach is that the local minima of the $\left[N_1 \times N_2\right]$- matrix of the logarithm are the proper guess values of the dispersion equation's roots. Hence all roots of Eqn. (17) could be found for values of wavenumbers $\left(k_i\right)$ on the real axis and on or near the imaginary axis as a function of frequency $\left(\omega_j\right)$. Another advantage of this method is that it is much faster than the traditional root finding methods and as fast as the method of Honarvar *et al.* (2008). The main disadvantage of this approach is that the roots of characteristic arguments ($\xi_k = 0,\ \left(k = 1,\ldots,4\right)$) are also displayed on the surface plots as obvious artefacts. An elaborate discussion of these artefacts is given in Yenwong-Fai (2008). These artefacts could be simply detected and eliminated from the dispersion plots by program tools. Our algorithm, as it has been implemented, does not search for branches of the dispersion relation well away from the real and imaginary axes for k. It would be relatively straightforward in principle to locate these additional branches.

Dispersion curves of bending waves $(m=1)$ in the cylinder made from PZT-4 with the short-circuit lateral (cylindrical) surface are depicted in Fig. 1 in dimensionless coordinates $\left[(k\cdot a)\div\Omega=\omega/(a\cdot V_s)\right]$, where $V_s=\sqrt{c_{44}^E/\rho}$, and a is the outer radius of the cylinder. The picture of the dispersion curves is obtained by a method described above for real (propagating waves) and pure imaginary values of the wavenumber in the limits $\mathrm{Re}(k\cdot a), \mathrm{Im}(k\cdot a)\in[0,8]$, $\Omega=\omega/(a\cdot V_s)\in[0,14]$ with resolution 500 (250 - for real and 250 – for imaginary $(k\cdot a)$) × 250 ($\omega/(a\cdot V_s)$) pixels. The same resolution is used for Fig. 2 – 17.

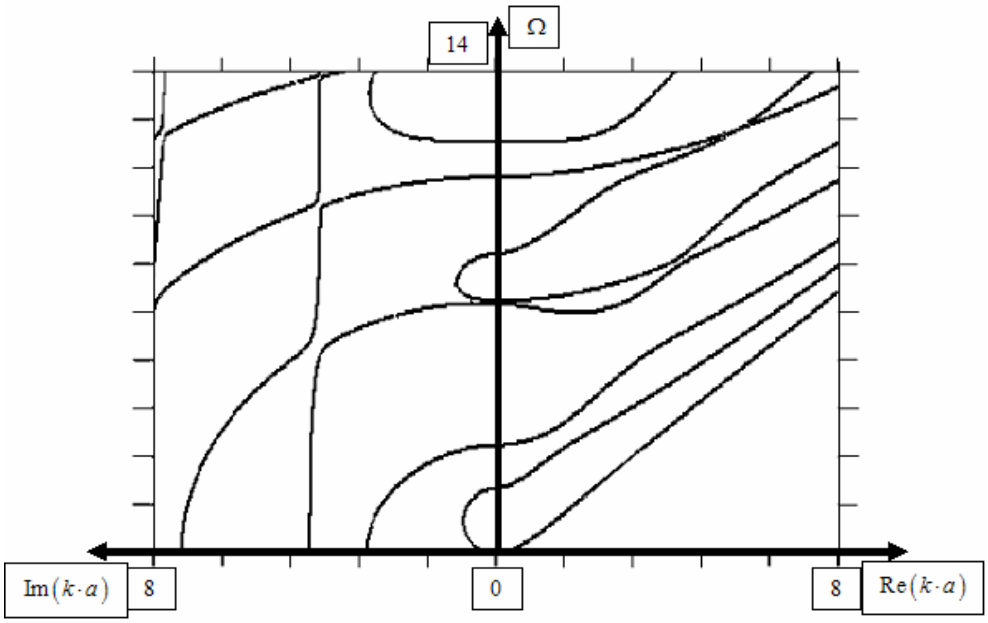

Fig. 1. PZT-4 cylinder with short-circuit lateral surface (m = 1)

The first dispersion curve of the propagating waves (real values of the wavenumber) tends to an asymptote of the surface wave propagation. It is joined to the second curve which tends to the asymptote of the shear waves through the domain of the evanescent waves. This picture does not correspond to the results obtained in Siao *et al.* (1994, Fig. 2, 3), where the second branch tends to an asymptote corresponding to a wave propagating with phase velocity which is approximately three times higher than the shear velocity. On the other hand our result is in full correspondence with the corresponding branch of *Bai et al.* (2004, Fig. 2), where the problem of wave propagation in a hollow piezoelectric cylinder was solved by a finite element method. Another mismatch between the results of the present paper and Siao *et al.* (1994, Fig. 2, 3) is in behaviour of the evanescent waves: our solution displays much steeper change of the dispersion curves. A similar steep behaviour of the dispersion curves is demonstrated by *Bai et al.* (2004, Fig. 2).

Dispersion curves of bending waves $(m=1)$ in the cylinder made from PZT-4 with the open-circuit lateral surface are demonstrated in Fig. 2. It is obvious that the electric boundary conditions substantially influence both propagating and evanescent

waves. For example, in the case of the open-circuit lateral surface the dispersion curves are even steeper than the corresponding curves in the case of the short-circuit lateral surface.

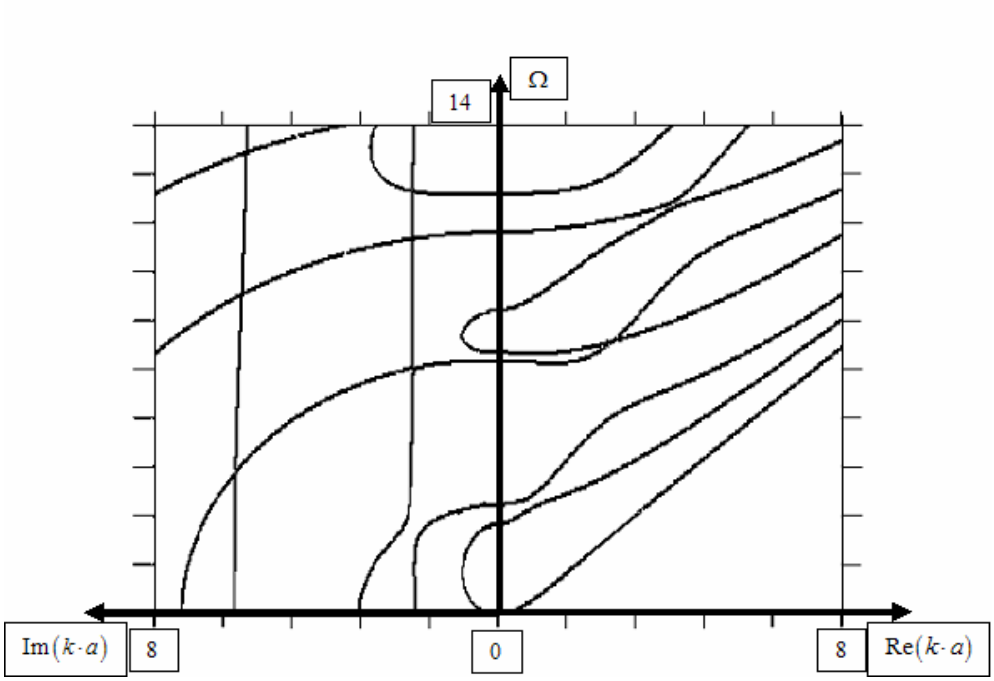

Fig. 2. PZT-4 cylinder with open-circuit lateral surface (m = 1)

In Fig. 3 a conceptual case of reduced electro-mechanical coupling coefficients $e_{15} = e_{31} = 0, e_{33} = 0.001 e_{33(PZT-4)}$ is shown.

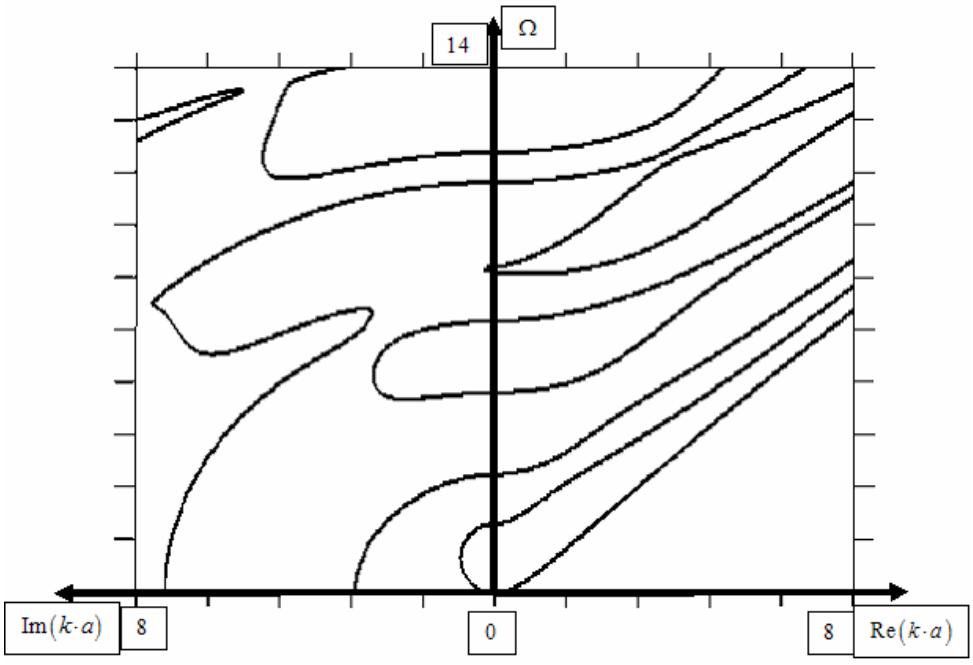

Fig. 3. PZT-4 cylinder with reduced electro-mechanical coupling
$\left(m = 1, \quad e_{15} = e_{31} = 0, e_{33} = 0.001 e_{33(PZT-4)}\right)$

In Fig. 4 and 5 the dispersion curves of PZT-7A material are presented for the open- and short-circuit lateral surfaces respectively. In comparison with PZT-4 this material has lower values of the electro-mechanical coupling coefficients but practically the same elastic coefficients and mass density.

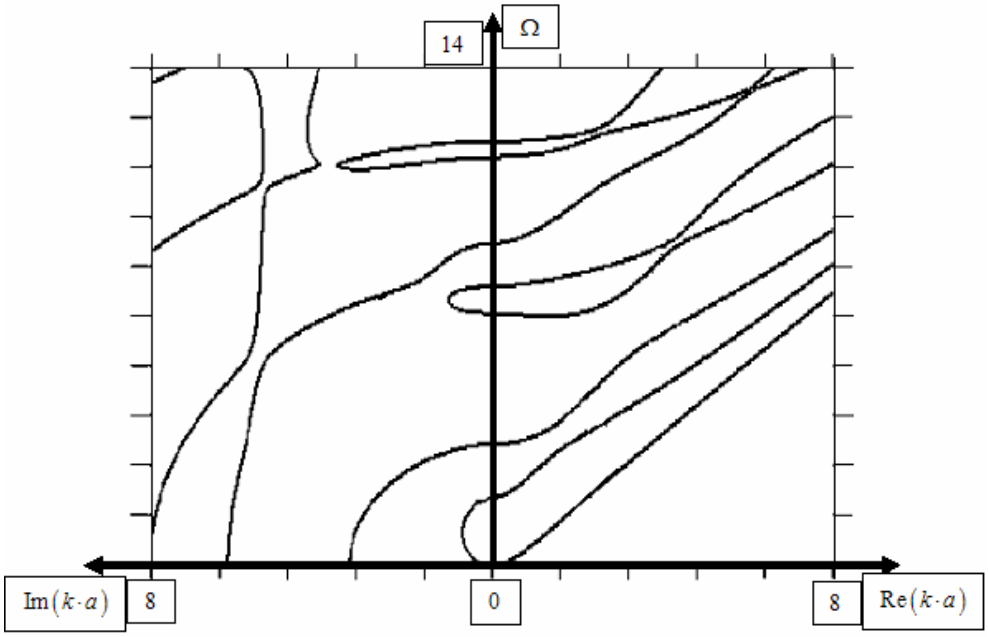

Fig. 4. PZT-7A cylinder with short-circuit lateral surface (m = 1)

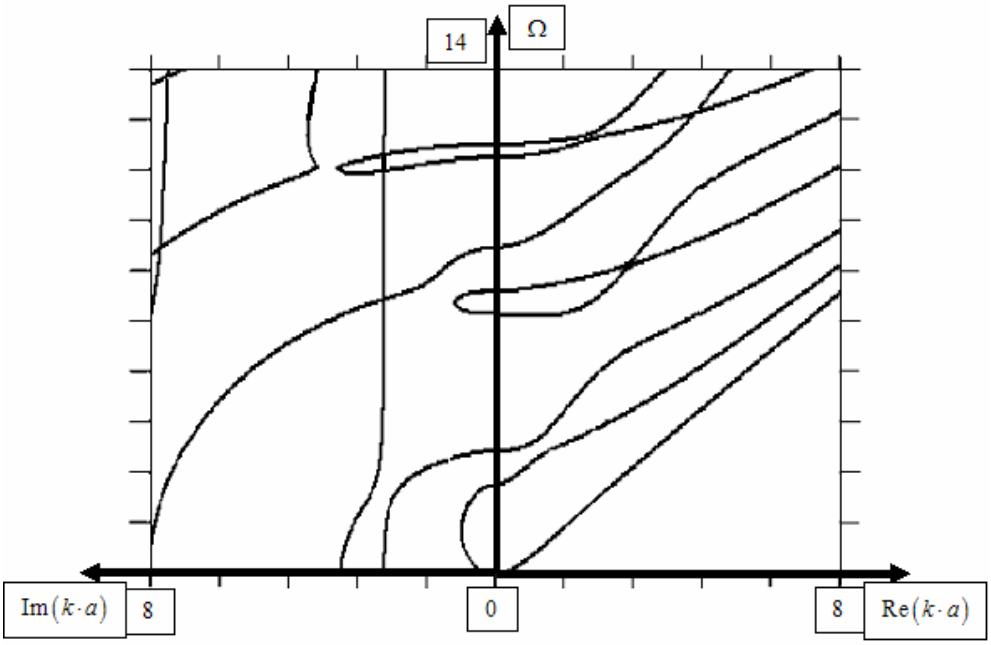

Fig. 5. PZT-7A cylinder with open-circuit lateral surface (m = 1)

It follows from Fig. 1 - 5 that the first fundamental mode of the bending waves is not sensitive to the nature of the electric boundary conditions on the lateral cylindrical surface. Furthermore it is practically not sensitive to the measure of electro-

mechanical coupling of the material. The higher order modes are more sensitive to the nature of the electric boundary condition as well as to the measure of the electro-mechanical cross-coupling. Fig. 3 - 5 shows that dispersion curves differ quite substantially from the curves in Fig. 1 and 2. This difference is explained mainly by the factor that the electro-mechanical coupling coefficients of PZT-7A are less than the corresponding factors of PZT-4. It is reflected in undulating behaviour of the propagating higher modes as well as the values of the cut-off frequencies. The PZT-4 cylinder with short-circuit lateral surface demonstrates a negative slope of the fourth branch in a quite broad range of wavenumbers (Fig. 1). Substantial dependence of dispersion curves on electric boundary conditions is obvious from the behaviour of the curves for the evanescent waves.

The phase velocities of the propagating waves for bending waves $(m=1)$ and short- and open-circuit lateral surface of the cylinders obtained from Fig. 1 - 2 and Fig. 4 - 5 are demonstrated in Fig. 6 – 9 for PZT-4 and PZT-7A.

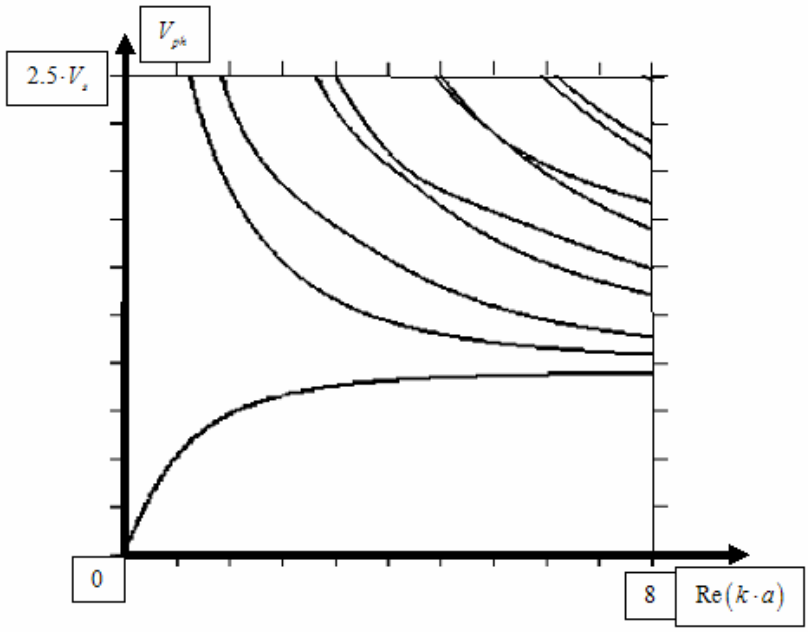

Fig. 6. Phase velocity in PZT-4 cylinder with short-circuit lateral surface (m = 1)

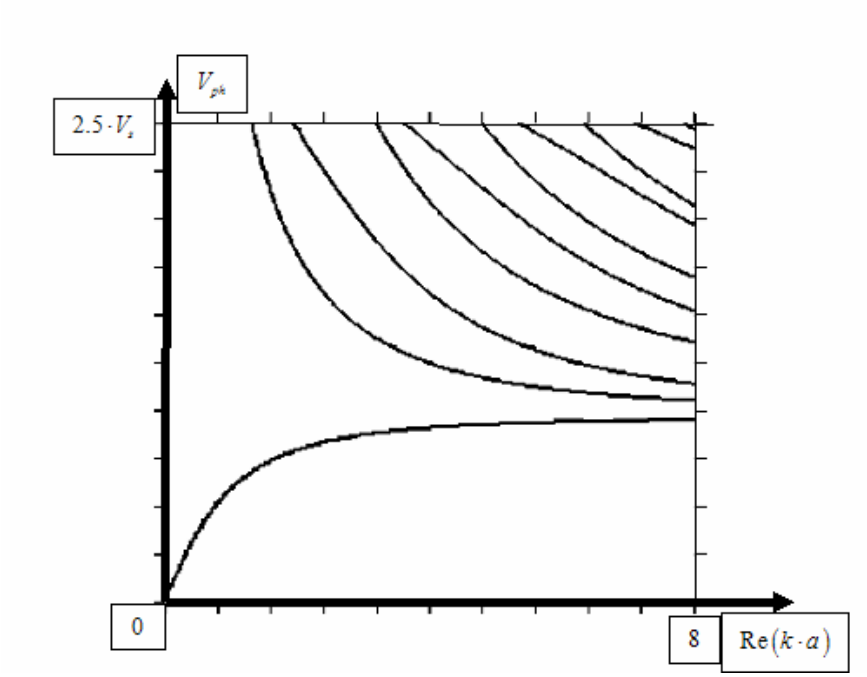

Fig. 7. Phase velocity in PZT4 cylinder with open-circuit lateral surface (m = 1)

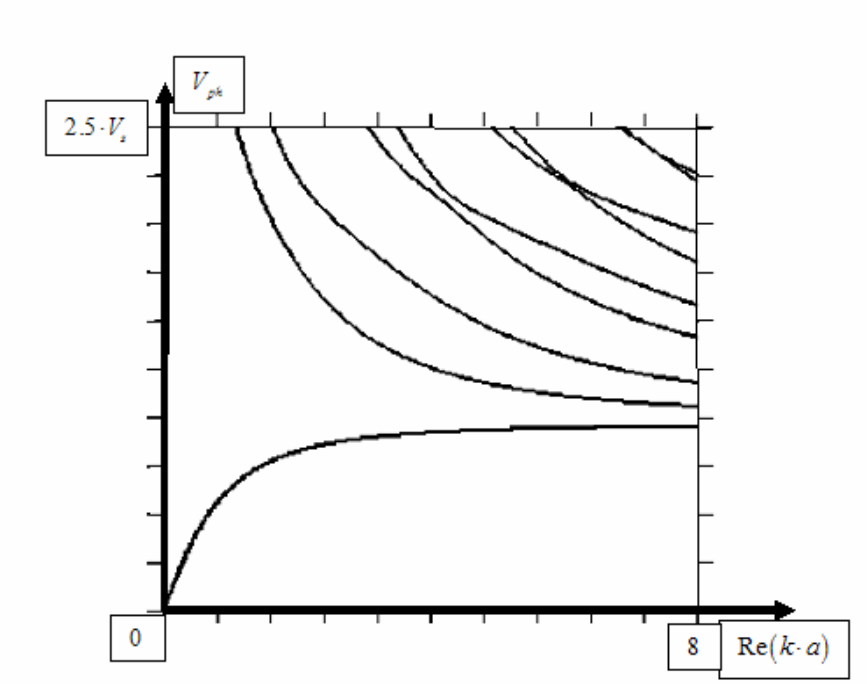

Fig. 8. Phase velocity in PZT7A cylinder with short-circuit lateral surface (m = 1)

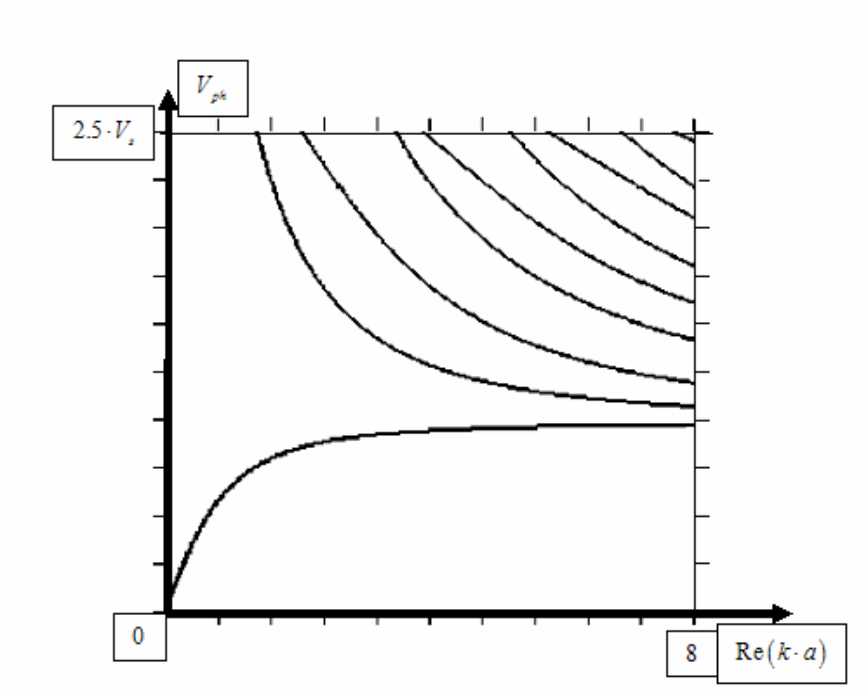

Fig. 9. Phase velocity in PZT7A cylinder with open-circuit lateral surface (m = 1)

Dispersion curves of non-axisymmetric waves with the circumferential wavenumber $m = 2$ in the cylinders made from PZT-4 and PZT-7A with the open- and close-circuit lateral surface are depicted in Fig. 10 - 13. Again as for the case $m = 1$ the substantial difference in the dispersion curves behaviour is explained by different types of the electric boundary conditions as well as by the difference in the electro-mechanic coupling coefficients.

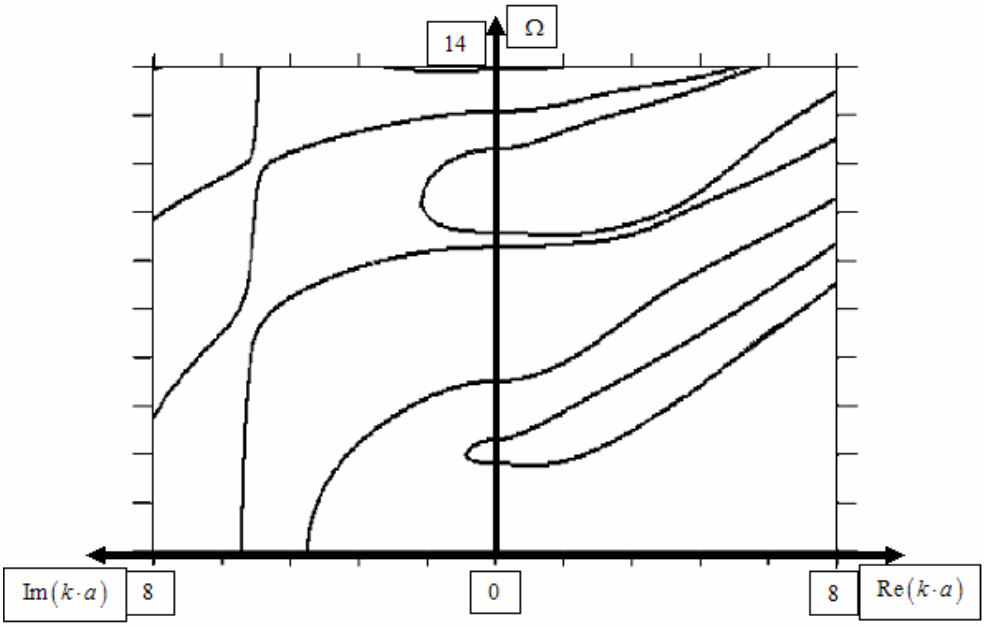

Fig. 10. PZT4 cylinder with short-circuit lateral surface (m = 2)

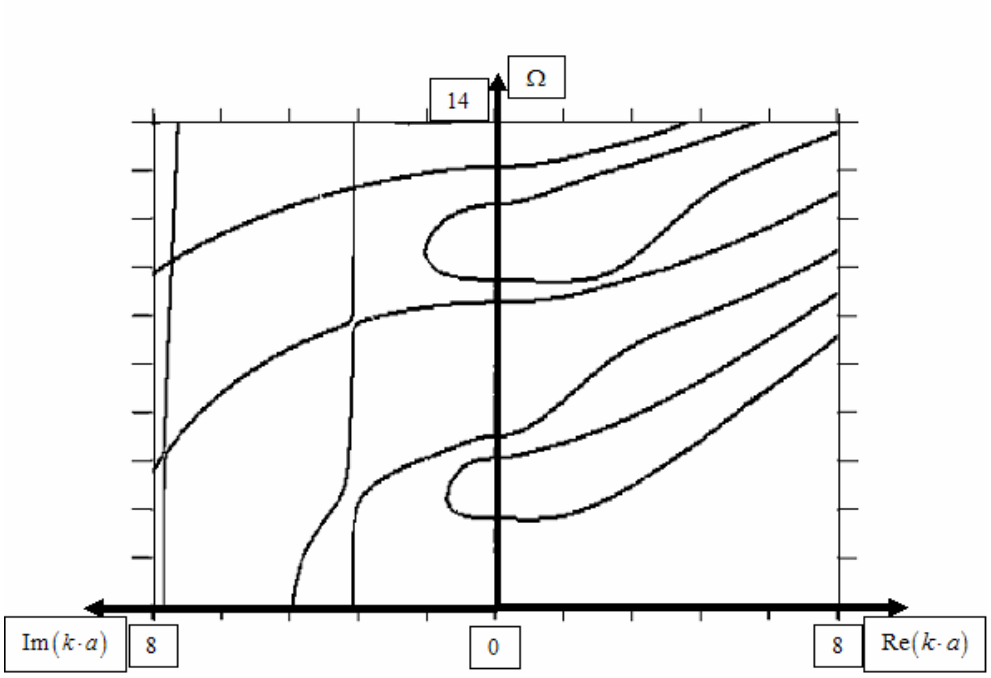

Fig. 11. PZT4 cylinder with open-circuit lateral surface (m = 2)

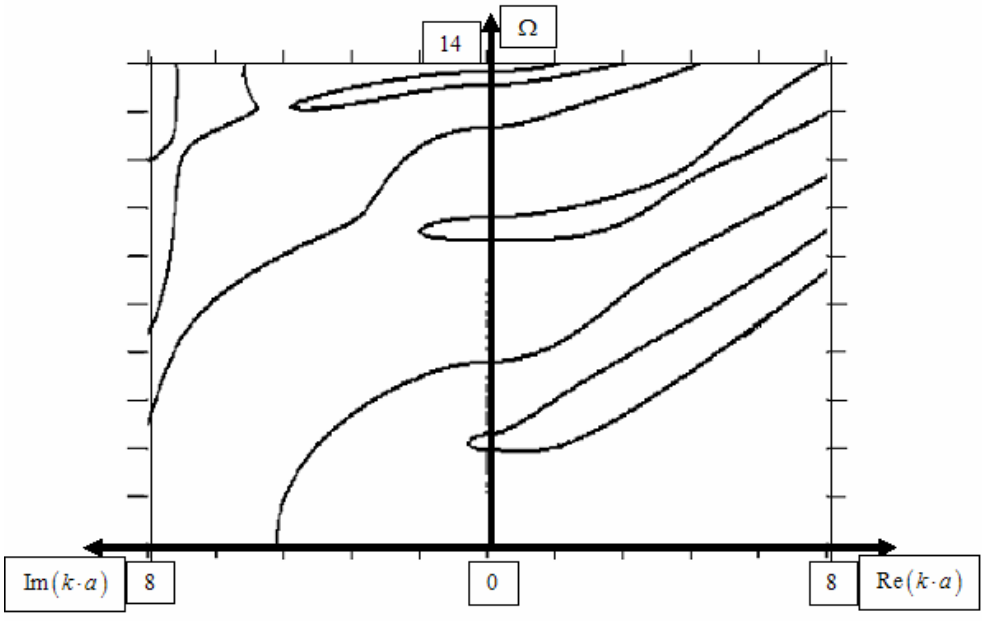

Fig. 12. PZT7A cylinder with short-circuit lateral surface (m = 2)

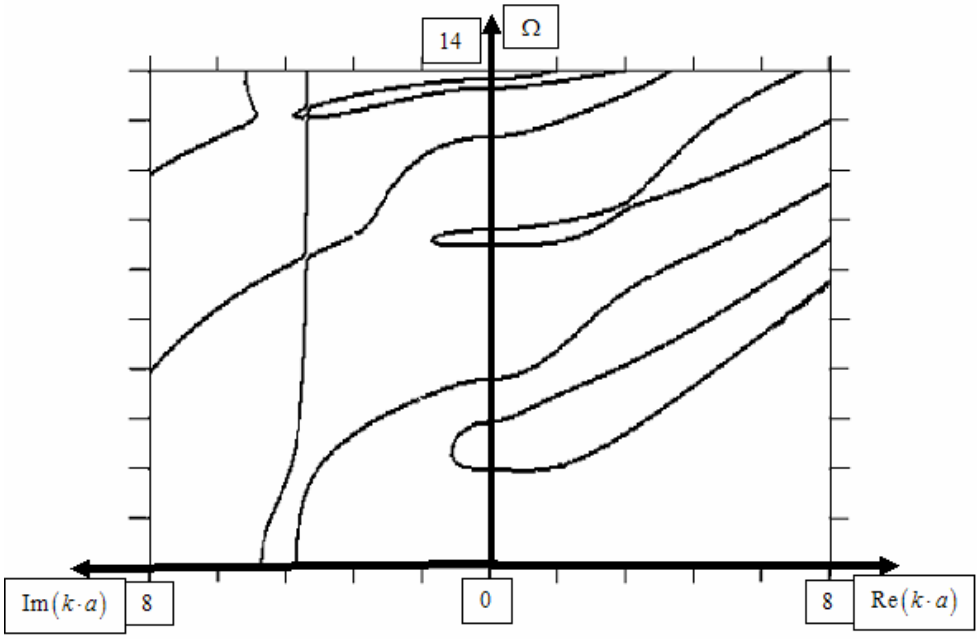

Fig. 13. PZT7A cylinder with open-circuit lateral surface (m = 2)

Dispersion curves of non-axisymmetric waves with the circumferential wavenumber $m = 3$ in the cylinder made from PZT-4 and PZT-7A with the open- and close-circuit lateral surface are depicted in Fig. 14-17.

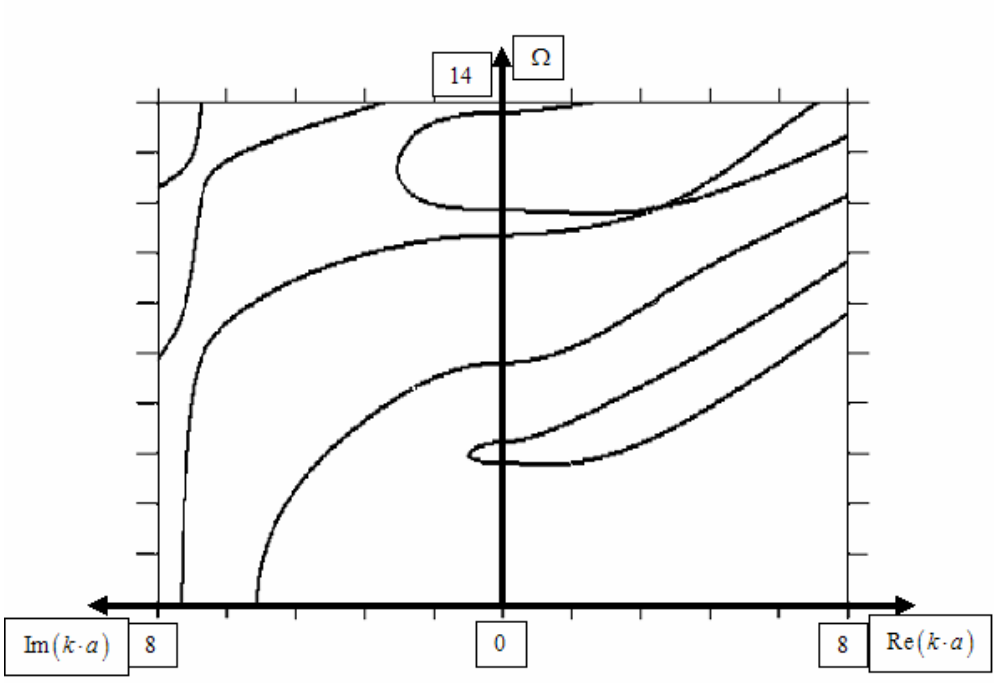

Fig. 14. PZT-4 cylinder with short-circuit lateral surface (m = 3)

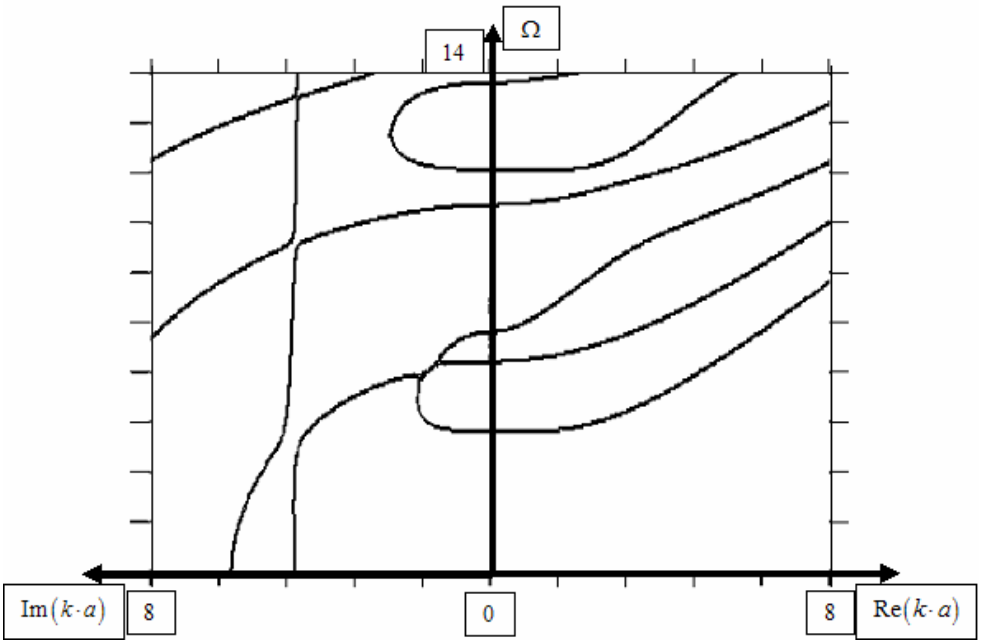

Fig. 15. PZT-4 cylinder with open-circuit lateral surface (m = 3)

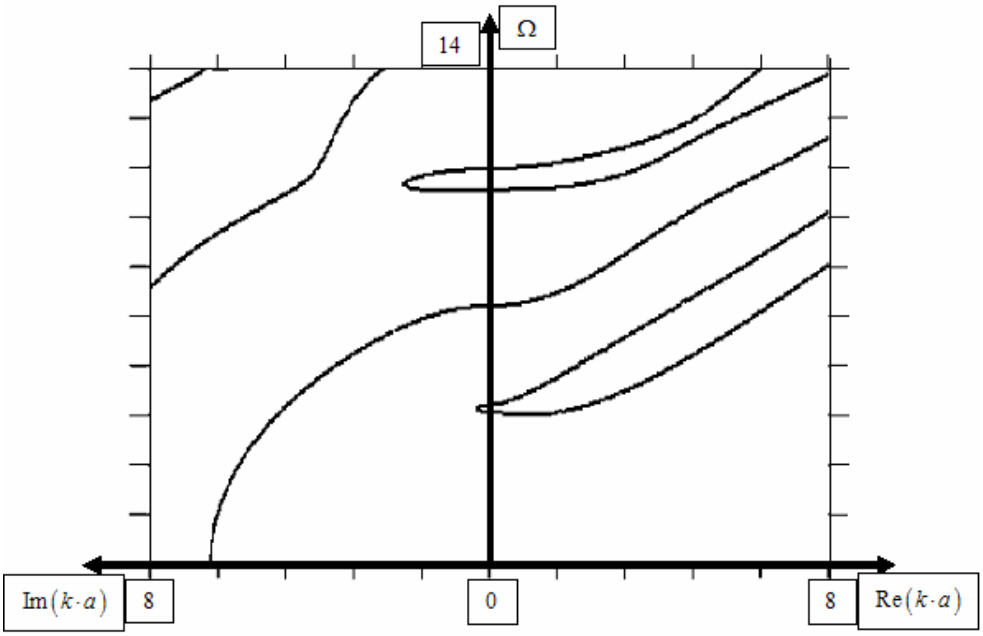

Fig. 16. PZT-7A cylinder with short-circuit lateral surface (m = 3)

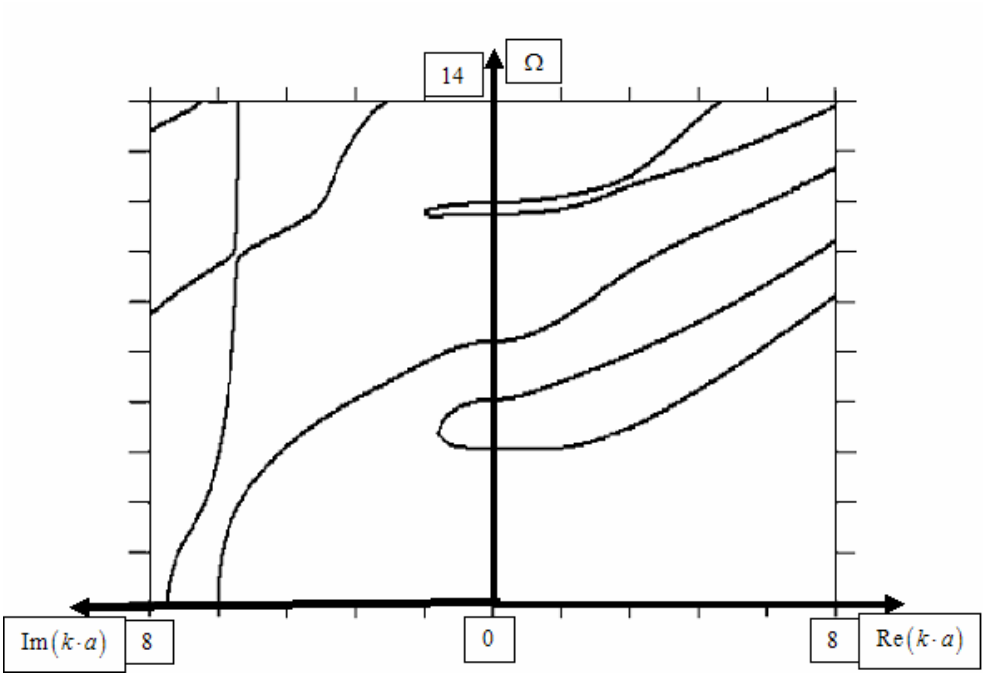

Fig. 17. PZT-7A cylinder with open-circuit lateral surface (m = 3)

The dispersion curves of higher circumferential wavenumbers $(m = 2, 3)$ are sensitive to the nature of the electric boundary condition as well as to the measure of the electro-mechanical cross-coupling for both propagating and evanescent waves. These dispersions curves obtained from the exact solution of the problem could be used as references data for developing of reliable finite elements for approximate solution of the problems of wave propagation in piezoelectric structures.

4 Summary

The characteristic equation of non-axisymmetric propagating and evanescent waves of a piezoelectric cylinder of transversely isotropic material was developed. The results were numerically illustrated for sample PZT-4 and PZT-7A cylinders for the first three circumferential wavenumbers $(m = 1, 2, 3)$. Phase velocities of the propagating waves were drawn for the bending mode $(m = 1)$. It was shown that the dispersion curves are sensitive both the electric boundary conditions and the measure of electro-mechanical coupling. This effect was revealed the more strongly in the higher order modes.

Appendix

Coefficients of the main determinant (17) for the case $\mathrm{Re}(\xi_j) \neq 0$, $(j = 1, \ldots, 4)$:

$$a_{11} = \frac{2\xi_1 c_{66}^E}{a} J_{m+1}(\xi_1 a) + \left[ik\left(\eta_1 c_{13}^E + \mu_1 e_{31}\right) - c_{11}^E \xi_1^2 + \frac{2c_{66}^E}{a^2} m(m-1) \right] J_m(\xi_1 a),$$

$$a_{21}=-\left[\left(\eta_1+ik\right)c_{44}^{E}+\mu_1 e_{15}\right]\left[\xi_1 J_{m+1}\left(\xi_1 a\right)-\frac{m}{a}J_m\left(\xi_1 a\right)\right],$$

$$a_{31}=\frac{2c_{66}^{E}m}{a}\left[\xi_1 J_{m+1}\left(\xi_1 a\right)-\frac{m-1}{a}J_m\left(\xi_1 a\right)\right],$$

$$a_{12}=\frac{2\xi_2 c_{66}^{E}}{a}J_{m+1}\left(\xi_2 a\right)+\left[ik\left(\eta_2 c_{13}^{E}+\mu_2 e_{31}\right)-c_{11}^{E}\xi_2^2+\frac{2c_{66}^{E}}{a^2}m\left(m-1\right)\right]J_m\left(\xi_2 a\right),$$

$$a_{22}=-\left[\left(\eta_2+ik\right)c_{44}^{E}+\mu_2 e_{15}\right]\left[\xi_2 J_{m+1}\left(\xi_2 a\right)-\frac{m}{a}J_m\left(\xi_2 a\right)\right],$$

$$a_{32}=\frac{2c_{66}^{E}m}{a}\left[\xi_2 J_{m+1}\left(\xi_2 a\right)-\frac{m-1}{a}J_m\left(\xi_2 a\right)\right],$$

$$a_{13}=\frac{2\xi_3 c_{66}^{E}}{a}J_{m+1}\left(\xi_3 a\right)+\left[ik\left(\eta_3 c_{13}^{E}+\mu_3 e_{31}\right)-c_{11}^{E}\xi_3^2+\frac{2c_{66}^{E}}{a^2}m\left(m-1\right)\right]J_m\left(\xi_3 a\right),$$

$$a_{23}=-\left[\left(\eta_3+ik\right)c_{44}^{E}+\mu_3 e_{15}\right]\left[\xi_3 J_{m+1}\left(\xi_3 a\right)-\frac{m}{a}J_m\left(\xi_3 a\right)\right],$$

$$a_{33}=\frac{2c_{66}^{E}m}{a}\left[\xi_3 J_{m+1}\left(\xi_3 a\right)-\frac{m-1}{a}J_m\left(\xi_3 a\right)\right],$$

$$a_{14}=-\frac{2mc_{66}^{E}}{a}\left[\xi_4 J_{m+1}\left(\xi_4 a\right)-\frac{m-1}{a}J_m\left(\xi_4 a\right)\right],\qquad a_{24}=\frac{imkc_{44}^{E}}{a}J_m\left(\xi_4 a\right),$$

$$a_{34}=-\frac{2c_{66}^{E}}{a}\left[\xi_4 J_{m+1}\left(\xi_4 a\right)-\left(\frac{\xi_4^2}{2}-\frac{m\left(m-1\right)}{a^2}\right)J_m\left(\xi_4 a\right)\right].$$

For the electric boundary condition $D_1\big|_{r=a}=0$, ($\mathrm{Re}\left(\xi_j\right)\neq 0$):

$$a_{41}=-\left[\left(\eta_1+ik\right)e_{15}-\mu_1\varepsilon_{11}^{S}\right]\left[\xi_1 J_{m+1}\left(\xi_1 a\right)-\frac{m}{a}J_m\left(\xi_1 a\right)\right],$$

$$a_{42}=-\left[\left(\eta_2+ik\right)e_{15}-\mu_2\varepsilon_{11}^{S}\right]\left[\xi_2 J_{m+1}\left(\xi_2 a\right)-\frac{m}{a}J_m\left(\xi_2 a\right)\right],$$

$$a_{43}=-\left[\left(\eta_3+ik\right)e_{15}-\mu_3\varepsilon_{11}^{S}\right]\left[\xi_3 J_{m+1}\left(\xi_3 a\right)-\frac{m}{a}J_m\left(\xi_3 a\right)\right],$$

$$a_{44}=\frac{imke_{15}}{a}J_m\left(\xi_4 a\right).$$

For the electric boundary condition $\phi\big|_{r=a}=0$, ($\mathrm{Re}\left(\xi_j\right)\neq 0$):

$$a_{41}=\mu_1 J_m\left(\xi_1 a\right),\qquad a_{42}=\mu_2 J_m\left(\xi_2 a\right),\qquad a_{43}=\mu_3 J_m\left(\xi_3 a\right),\qquad a_{44}=0.$$

Coefficients of the main determinant (17) for the case $\mathrm{Re}\left(\xi_j\right)=0$, $\left(j=1,\ldots,4\right)$:

$$a_{11}=-\frac{2\left|\xi_1\right|c_{66}^{E}}{a}I_{m+1}\left(\left|\xi_1\right|a\right)+\left[ik\left(\eta_1 c_{13}^{E}+\mu_1 e_{31}\right)+c_{11}^{E}\left|\xi_1\right|^2+\frac{2c_{66}^{E}}{a^2}m\left(m-1\right)\right]I_m\left(\left|\xi_1\right|a\right),$$

$$a_{21}=\left[\left(\eta_1+ik\right)c_{44}^{E}+\mu_1 e_{15}\right]\left[\left|\xi_1\right|I_{m+1}\left(\left|\xi_1\right|a\right)+\frac{m}{a}I_m\left(\left|\xi_1\right|a\right)\right],$$

$$a_{31}=-\frac{2c_{66}^{E}m}{a}\left[\left|\xi_1\right|I_{m+1}\left(\left|\xi_1\right|a\right)+\frac{m-1}{a}I_m\left(\left|\xi_1\right|a\right)\right],$$

$$a_{12}=-\frac{2\left|\xi_2\right|c_{66}^{E}}{a}I_{m+1}\left(\left|\xi_2\right|a\right)+\left[ik\left(\eta_2 c_{13}^{E}+\mu_2 e_{31}\right)+c_{11}^{E}\left|\xi_2\right|^2+\frac{2c_{66}^{E}}{a^2}m\left(m-1\right)\right]I_m\left(\left|\xi_2\right|a\right),$$

$$a_{22}=\left[\left(\eta_2+ik\right)c_{44}^{E}+\mu_2 e_{15}\right]\left[\left|\xi_2\right|I_{m+1}\left(\left|\xi_2\right|a\right)+\frac{m}{a}I_m\left(\left|\xi_2\right|a\right)\right],$$

$$a_{32}=-\frac{2c_{66}^{E}m}{a}\left[\left|\xi_2\right|I_{m+1}\left(\left|\xi_2\right|a\right)+\frac{m-1}{a}I_m\left(\left|\xi_2\right|a\right)\right],$$

$$a_{13}=-\frac{2\left|\xi_3\right|c_{66}^{E}}{a}I_{m+1}\left(\left|\xi_3\right|a\right)+\left[ik\left(\eta_3 c_{13}^{E}+\mu_3 e_{31}\right)+c_{11}^{E}\left|\xi_3\right|^2+\frac{2c_{66}^{E}}{a^2}m\left(m-1\right)\right]I_m\left(\left|\xi_3\right|a\right),$$

$$a_{23}=\left[\left(\eta_3+ik\right)c_{44}^{E}+\mu_3 e_{15}\right]\left[\left|\xi_3\right|I_{m+1}\left(\left|\xi_3\right|a\right)+\frac{m}{a}I_m\left(\left|\xi_3\right|a\right)\right],$$

$$a_{33}=-\frac{2c_{66}^{E}m}{a}\left[\left|\xi_3\right|I_{m+1}\left(\left|\xi_3\right|a\right)+\frac{m-1}{a}I_m\left(\left|\xi_3\right|a\right)\right],$$

$$a_{14}=\frac{2mc_{66}^{E}}{a}\left[\left|\xi_4\right|I_{m+1}\left(\left|\xi_4\right|a\right)+\frac{m-1}{a}I_m\left(\left|\xi_4\right|a\right)\right],\qquad a_{24}=\frac{imkc_{44}^{E}}{a}I_m\left(\left|\xi_4\right|a\right),$$

$$a_{34}=\frac{2c_{66}^{E}}{a}\left[\left|\xi_4\right|I_{m+1}\left(\left|\xi_4\right|a\right)-\left(\frac{\left|\xi_4\right|^2}{2}+\frac{m\left(m-1\right)}{a^2}\right)I_m\left(\left|\xi_4\right|a\right)\right].$$

For the electric boundary condition $D_1\big|_{r=a}=0$, ($\mathrm{Re}\left(\xi_j\right)=0$):

$$a_{41}=\left[\left(\eta_1+ik\right)e_{15}-\mu_1\varepsilon_{11}^{S}\right]\left[\left|\xi_1\right|I_{m+1}\left(\left|\xi_1\right|a\right)+\frac{m}{a}I_m\left(\left|\xi_1\right|a\right)\right],$$

$$a_{42}=\left[\left(\eta_2+ik\right)e_{15}-\mu_2\varepsilon_{11}^{S}\right]\left[\left|\xi_2\right|I_{m+1}\left(\left|\xi_2\right|a\right)+\frac{m}{a}I_m\left(\left|\xi_2\right|a\right)\right],$$

$$a_{43}=\left[\left(\eta_3+ik\right)e_{15}-\mu_3\varepsilon_{11}^{S}\right]\left[\left|\xi_3\right|I_{m+1}\left(\left|\xi_3\right|a\right)+\frac{m}{a}I_m\left(\left|\xi_3\right|a\right)\right],$$

$$a_{44}=\frac{imke_{15}}{a}I_m\left(\left|\xi_4\right|a\right).$$

For the electric boundary condition $\phi\big|_{r=a}=0$, ($\mathrm{Re}\left(\xi_j\right)=0$):

$$a_{41}=\mu_1 I_m\left(\left|\xi_1\right|a\right),\qquad a_{42}=\mu_2 I_m\left(\left|\xi_2\right|a\right),\qquad a_{43}=\mu_3 I_m\left(\left|\xi_3\right|a\right),\qquad a_{44}=0.$$

References

Achenbach, J., 1984. Wave Propagation in Elastic Solids. New York, North-Holland.

Armenakas, A., Reitz, E., 1973. Propagation of harmonic waves in orthotropic circular cylindrical shells. J. Appl. Mech. 40, 168-174.

Bai, H., Shah, A., Dong, S., Taciroglu, E., October 2006. End reflections in layered piezoelectric circular cylinder. International Journal of Solids and Structures, 43, 6309-6325.

Bai, H., Taciroglu, E., Dong, S., Shah, A., June 2004. Elastodynamic Green's function for a laminated piezoelectric cylinder. International Journal of Solids and Structures, 41, 6335–6350.

Berliner, M., Solecki, R., Wave propagation in fluid-loaded transversely isotropic cylinders. Part 1. Analytical formulation. J. Acoust. Soc. Am., 99, 1841-1847.

Chree, C., 1890. Q. J. Math. 24, 340-354.

Crandall, S., Karnop, E., Kurtz, J., Pridemore-Brown, D., 1968. Dynamics of Mechanical and Electromechanical Systems. Krieger Publishing Co, Malabar, Florida.

Every A., Neiman V., 1992. Reflection of electroacoustic waves in piezoelectric solids: Mode conversion into four bulk waves. J. Appl. Phys. 71, 6018-6024.

Frazer, W., 1980. Separable equations for a cylindrical anisotropic elastic waveguide. J. Sound Vib. 72, 151-157.

Graff K., 1991. Wave Motion in Elastic Solids. New York: Dover.

Hagood, N., Chung, W., Flotow, A., 1990. Modelling of piezoelectric actuator dynamics for active structural control. J. of Intell. Mater. Syst. And Struct. 1 (3), 327-354.

Honarvar, F., Enjilela, E., Sinclair, A., 2008. An alternative method for plotting dispersion curves, Ultrasonics , doi:10.1016/ j.ultras.2008.07.002

Honarvar, F., Enjilela, E., Sinclair, A., Minerzami, S., 2007. Wave propagation in transversely isotropic cylinders. International Journal of Solids and Structures, 44, 5236-5246.

Mirsky, I., 1964. Wave propagation in transversely isotropic circular cylinders. Part 1: Theory. J. Acoust. Soc. Am. 36, 2106-2122.

Nayfeh, A., Abdelrahman, W., Nagy, P., 2000. Analysys of axisymmetric waves in layered piezoelectric rods and their composites. J. Acoust. Soc. Am. 108 (4), 1496-1504.

Nayfeh. A., Nagy, P., 1995. General study of axisymmetric waves in layered anisotropic fibres and their composites. J. Acoust. Soc. Am., 99, 931-941

Niklasson, A., Datta, S., 1998. Scattering by an infinite transversely isotropic cylinder in a transversely isotropic medium. Wave motion 27 (2), 169-185.

Paul, H., 1966. Vibrations of circular cylindrical shells of piezoelectric silver iodide crystals. J. Acoust. Soc. Am. 40, 1077-1080.

Pochhammer, L., 1876. J. reine angew. Math. 81, 324.

Rose, J., 1999. Ultrasonic Waves in Solid Media. Cambridge University Press.

Shatalov, M., Loveday, P., 2004. Electroacoustic wave propagation in transversely isotropic piezoelectric cylinders. Proceedings of the South African Conference on Applied Mechanics (SACAM04).

Siao, J., Dong, S., Song, J., 1994. Frequency spectra of laminated piezoelectric cylinders. ASME Journal of Vibrations and Acoustics 116, 364-370.

Wei, J., Su, X., 2005. Wave propagation in a piezoelectric rod of 6mm symmetry. International Journal of Solids and Structures, 42, 3644-3654.

Winkel, V., oliveira, J., Dai, J., Jen, C., 1995. Acoustic wave propagation in piezoelectric fibres of hexagonal crystall symmetry. IEEE Trans. Ultrason. Ferroelectr. Freq. Control 42, 949-955.

Xu, P., Datta, S., 1991. Characterization of fibre-matrix interface by guided waves: Axisymmetric case. J. Acoust. Soc. Am 89 (6), 2573-2583.

Yenwong-Fai, A., 2008. Wave propagation in a piezoelectric solid cylinder of transversely isotropic material. Master's thesis, University of Witwatersrand, Johannesburg, South Africa.